frontiers | Frontiers in Built Environment

TYPE Brief Research Report
PUBLISHED 18 August 2025
DOI 10.3389/fbuil.2025.1662269

OPEN ACCESS

EDITED BY
Jie Han,
University of Kansas, United States

REVIEWED BY
Junliang Tao,
Arizona State University, United States
Hai Lin,
Louisiana State University, United States

*CORRESPONDENCE
Michael G. Gomez,
mggomez@uw.edu

RECEIVED 08 July 2025
ACCEPTED 06 August 2025
PUBLISHED 18 August 2025

CITATION
Gomez MG, Martinez EM, Ribeiro BGO and Tai C-E (2025) Investigating air entrapment in biocemented composites for geotechnical ground improvement.
Front. Built Environ. 11:1662269.
doi: 10.3389/fbuil.2025.1662269

Investigating air entrapment in biocemented composites for geotechnical ground improvement

Michael G. Gomez*, Erick M. Martinez, Bruna G. O. Ribeiro and Chung-En Tai

Department of Civil and Env. Engineering, University of Washington, Seattle, WA, United States

Biocementation is a biomediated ground improvement method that can improve the engineering behavior of granular soils through the precipitation of calcium carbonate minerals. Although cemented bonds and particle coatings generated from biocementation can enable large increases in soil initial shear stiffness, peak shear strength, and liquefaction resistance; emerging strategies such as soil desaturation have shown the ability of alternative mechanisms to enable large improvements in liquefaction behaviors. This article highlights outcomes from recent experiments which have investigated the potential of novel treatment processes to enable the generation and entrapment of gases within biocementation. We hypothesize that these entrapped gases may provide a secondary mechanism to improve soil undrained shearing behaviors by enabling the release of gases following cemented bond deterioration and related increases in pore fluid compressibility. Our study employs a series of batch experiments to identify new methods to both generate and entrap gasses within an organic polymer layer applied intermittently between biocementation treatments. Biocemented composites resulting from this work may enable large improvements in the environmental and financial efficacy of biocementation and the resilience of treated soils to extreme loading events.

KEYWORDS

MICP, calcite, geotechnical engineering, soil improvement, biocementation, biomediated, ground improvement

Introduction

Geotechnical ground improvement is an over 6 billion dollar per year industry in the U.S. that has relied almost exclusively on energy-intensive materials (e.g., portland cement) and high mechanical energy to improve problematic soils (DeJong et al., 2010; Mitchell and Kelly, 2013). Over nearly 2 decades, researchers have shown the potential of biomediated processes to enable improvements in soil engineering behaviors with the potential to minimize environmental impacts (Ferris et al., 1997; Stocks-Fischer et al., 1999; DeJong et al., 2013). Calcium carbonate ($CaCO_3$) mineral precipitation methods are the most widely researched biomediated soil improvement processes, with precipitation commonly achieved through microbial urea hydrolysis, in a process known as Microbially Induced

Calcite Precipitation (MICP) (DeJong et al., 2022). Biocementation can transform the engineering behavior of soils with a variety of different geotechnical applications including liquefaction mitigation, erosion control, and foundation capacity improvement (DeJong et al., 2022).

Although most studies have investigated behaviors afforded by high levels of biocementation, recent studies suggest that even very light levels of biocementation (<1% $CaCO_3$) can afford dramatic improvements in liquefaction behaviors. For example, 0.5% $CaCO_3$ by mass can increase the liquefaction resistance of loose clean sands by over 100 times at low loading magnitudes (CSR <0.15), suggesting that the resources and costs associated with conventional soil improvement may be greatly reduced (Lee and Gomez, 2024). While encouraging, these same lightly biocemented soils exhibit minimal improvements in larger-strain behaviors observed after triggering (i.e., post-triggering strain accumulation, reconsolidation strains) with unfavorable responses including rapid strength and stiffness losses post-peak and shear localization also observed during monotonic loading (Montoya and DeJong, 2015; Feng and Montoya, 2016; Lee and Gomez, 2024). Higher magnitudes of biocementation can be used to effectively "densify" soils and achieve greater improvements at larger strains, however, generating high levels of cementation may necessitate significant adverse economic and environmental impacts. Instead, modifications to the material structure and composition of biocementation may afford new opportunities to improve soil engineering response while maximizing process efficacy.

Concurrent with advances in biocementation, there has been significant recent research interest in the use of soil desaturation as an alternative soil improvement mechanism. The process can enable large improvements in soil undrained shearing behaviors and liquefaction resistances by reducing excess pore pressure generation typically observed in contractive loose-of-critical soils during shearing. Understandings of improvements afforded by this process come from both experiments involving abiotic gas injections as well as biologically induced mechanisms such as microbial denitrification. For example, Okamura and Soga (2006) used abiotic gas injections and found that greater than one order of magnitude improvement in soil liquefaction resistances could be achieved with a small decrease in soil saturation ratios from 100% to 98%. He et al. (2014) observed large increases in liquefaction resistance with desaturation induced by biogas production in shake table tests. Studies by van Paassen et al. (2010), O'Donnell et al. (2017), Pham et al. (2018), Zeng et al. (2022), Sorenson et al. (2022) and many others have further investigated how the process can be optimized and deployed at field-scale and have also characterized related improvements in undrained shearing behaviors. An opportunity exists to leverage this mechanism and develop novel biocemented composite materials which contain entrapped gases.

In this study, a series of batch experiments were employed to specifically investigate the potential of gases to be generated and entrapped within biocemented composite materials. We hypothesize that these biocemented composites will provide a secondary mechanism to improve soil undrained behaviors by releasing trapped gases following cemented bond damage, increasing pore fluid compressibility, and therefore achieving improved shearing behaviors at larger strains where conventional biocementation is less effective. All experiments were designed to explore treatment processes wherein soils were first biocemented, a second treatment was applied consisting of a solution with biopolymers and fermentable substrates to initiate microbial mixed acid fermentation (MAF) and mineral dissolution to generate and retain carbon dioxide gases at the surface of calcium carbonate crystals, and a third treatment was applied to coat polymer layers containing generated gases with additional biocementation to retain these layers within the biocemented composite. Batch experiments first examined effects imparted by biocementation (referred to as "MICP") and subsequent polymer and MAF treatments (referred to as "PolyMAF") on sand microstructures to identify methods that could generate and retain gases at crystal surfaces. Following this, subsequent batch experiments explored the ability of secondary cementation treatments to effectively coat gas containing polymer layers with additional cementation to achieve a composite with entrapped gases. Results from select experiments are presented including scanning electron microscope (SEM) images of intact soils and material cross-sections as well as scanning electron microscopy with energy dispersive x-ray spectroscopy (SEM-EDS) scans used to characterize element spatial abundances. Biocemented composites identified through this work may enable large improvements in the efficacy of biocementation and its resilience to extreme loading events.

Materials and methods

Batch experiments

Batch experiments were conducted following procedures similar to Burdalski et al. (2022) in 100 mm diameter, 15 mm high flat bottom glass dishes containing 5.3 g of Ottawa F65 sand and 44 mL of aqueous solutions. Ottawa F65 sand is a clean poorly graded quartz sand with a D_{50} of 0.21 mm and no fines (Carey et al., 2020) that has been used extensively in biocementation experiments.

Augmentation and MAF inoculant

All batch experiments were augmented with *S. pasteurii* (ATCC 11859) cells to enable urea hydrolysis and biocementation. Cells were augmented prior to the first cementation treatment as well as before secondary cementation treatments, when present. During the first augmentation event, dry sand masses were vortexed with concentrated and rinsed *Sporosarcina pasteurii* cells pellets in a plastic 50 mL conical tube and allowed to reside for at least 24 h prior to experiments to enable cell attachment. During the second augmentation event, an identical procedure was used with moist sand after discarding the previous solution. At the start of experiments, the augmented sand and cell mixture was poured into a glass dish and cementation solutions were subsequently added to mimic biocementation treatment processes. Cells were grown in growth media (15.74 g/L Tris Base, 20 g/L yeast extract, 10 g/L ammonium sulfate, pH adjusted to 9.0) following procedures described in Burdalski et al. (2022) from a frozen glycerol stock culture. All cells were centrifuged and rinsed with sterile isotonic saline solution prior to use in experiments to minimize the

presence of possible growth factors. All experiments had a *S. pasteurii* cell density near 7×10^7 cells/mL during cementation treatments. Cell inoculants for mixed acid fermentation (MAF) treatments were prepared via stimulation of a native sand following procedures described in Gomez et al. (2023) wherein a solution containing glucose and yeast extract was supplied to a natural sand under limited oxygen conditions and reductions in pH were monitored to assess fermentation activity prior to use. Although other acid generation mechanisms could have been used, mixed acid fermentation was selected to enable the release both carbon dioxide gasses and calcium ions during the dissolution of calcium carbonate minerals and the generation of additional carbon dioxide as a fermentation byproduct.

Treatment schemes

Eight batch experiments were performed to investigate various aspects of the treatment process. Experiments received treatments in the following phases: (i) augmentation, cementation, and post-treatment rinse solutions, (ii) polymer and fermentable substrate and post-treatment rinse solutions, and (iii) secondary augmentation, cementation, and post-treatment rinse solutions. In order to isolate specific effects, some of the above treatment phases were modified and/or removed in select experiments as described below. All solutions were prepared with deionized water and all experiments contained only Ottawa F65 sand as the soil. All cementation and PolyMAF treatments were allowed to reside for 72 h after application. All experiments had similar reaction rates as evaluated by urea concentration measurements in time during cementation treatments.

Series 1 experiments (Experiments 1 through 3) explored the effect of MICP and PolyMAF treatments on the baseline sand. Experiment 1 referred to as "Uncemented Ottawa F65" consisted of only untreated Ottawa F65 sand to establish baseline soil morphologies. Experiment 2 referred to as "MICP Treated Ottawa F65" received only an initial augmentation and cementation treatment (250 mM urea, 250 mM calcium chloride, 0.2 g/L yeast extract) followed by rinsing with 35% ethanol to remove treatment byproducts to establish expected microstructures after biocementation. Experiment 3 referred to as "MICP Treated Ottawa F65 w/PolyMAF" received an initial augmentation and cementation treatment (250 mM urea, 250 mM calcium chloride, 0.2 g/L yeast extract) followed by rinsing with 35% ethanol to remove treatment byproducts and a PolyMAF treatment (0.005% by mass sodium alginate, 10 g/L glucose, 1 g/L yeast extract, 0.33% by volume of MAF inoculant) to establish the effects of the PolyMAF treatment applied after biocementation. Sodium alginate was specifically selected for the PolyMAF treatment following preliminary testing due to its ability to (i) trap gas bubbles yet maintain a low enough viscosity at the concentrations used to permit injections in porous media and (ii) form a stiffer calcium alginate gel in the presence of calcium ions released from dissolution.

Series 2 experiments (Experiments 4 through 8) further explored gas entrapment and coating by a secondary cementation treatment. All series 2 experiments were first augmented and received a cementation treatment (250 mM urea and 250 mM calcium chloride) followed by rinsing with 35% ethanol to remove treatment byproducts before subsequent treatments. When present, all PolyMAF treatments contained 0.01% by mass sodium alginate, 10 g/L glucose, 1 g/L yeast extract, and 0.33% by volume of MAF inoculant. Experiment 4 referred to as "MICP–No PolyMAF–MICP" received an initial augmentation and cementation treatment followed by rinsing and a second augmentation and cementation treatment (250 mM urea, 250 mM calcium chloride) with no PolyMAF treatment. Experiment 5 referred to as "MICP–PolyMAF–MICP" received an initial augmentation and cementation treatment followed by rinsing, a PolyMAF treatment, decanting to remove reacted PolyMAF, and augmentation and secondary cementation treatments (250 mM urea, 250 mM calcium chloride). Experiment 6 referred to as "MICP–PolyMAF–MICP w/50 mM Mg^{2+}" received an initial augmentation and cementation treatment followed by rinsing, a PolyMAF treatment, decanting to remove reacted PolyMAF, and augmentation and secondary cementation treatments with added magnesium (250 mM urea, 250 mM calcium chloride, 50 mM magnesium chloride). Experiment 7 referred to as "MICP–PolyMAF–MICP w/250 mM Mg^{2+}" received an initial augmentation and cementation treatment followed by rinsing, a PolyMAF treatment, decanting to remove reacted PolyMAF, and a second augmentation and cementation treatment with higher added magnesium (250 mM urea, 250 mM calcium chloride, 250 mM magnesium chloride). Finally, Experiment 8 referred to as "MICP–No PolyMAF–MICP w/50 mM Mg^{2+}" received an initial augmentation and cementation treatment followed by rinsing, and a second augmentation and cementation treatment with added magnesium (250 mM urea, 250 mM calcium chloride, 50 mM magnesium chloride) with no PolyMAF treatments.

SEM imaging and sample cross sectioning

After all treatments, solutions were decanted and discarded from batch experiments and remaining biocemented samples were rinsed with 70% ethanol and oven dried. Dry soil subsamples were then prepared for SEM imaging by mounting onto a pedestal with carbon tape and sputter coating with platinum. For select samples, scanning electron microscopy with energy dispersive x-ray spectroscopy (SEM-EDS) was also performed to examine elemental compositions. Select soil subsamples were epoxied and cross sectioned prior to imaging to examine internal structures to assess the generation and entrapment of gasses within biocemented composites. Samples were cross sectioned by embedding samples within a hard epoxy, slow sawing after curing using a diamond wafer microblade, and extensively polishing prior to imaging. SEM images presented in this study were selected to be as representative as possible of most locations within samples.

Results

Series 1 experiments

Series 1 experiments characterized changes in sand microstructure resulting from MICP and a PolyMAF treatment after MICP. Figure 1 provides SEM images of intact soil subsamples from

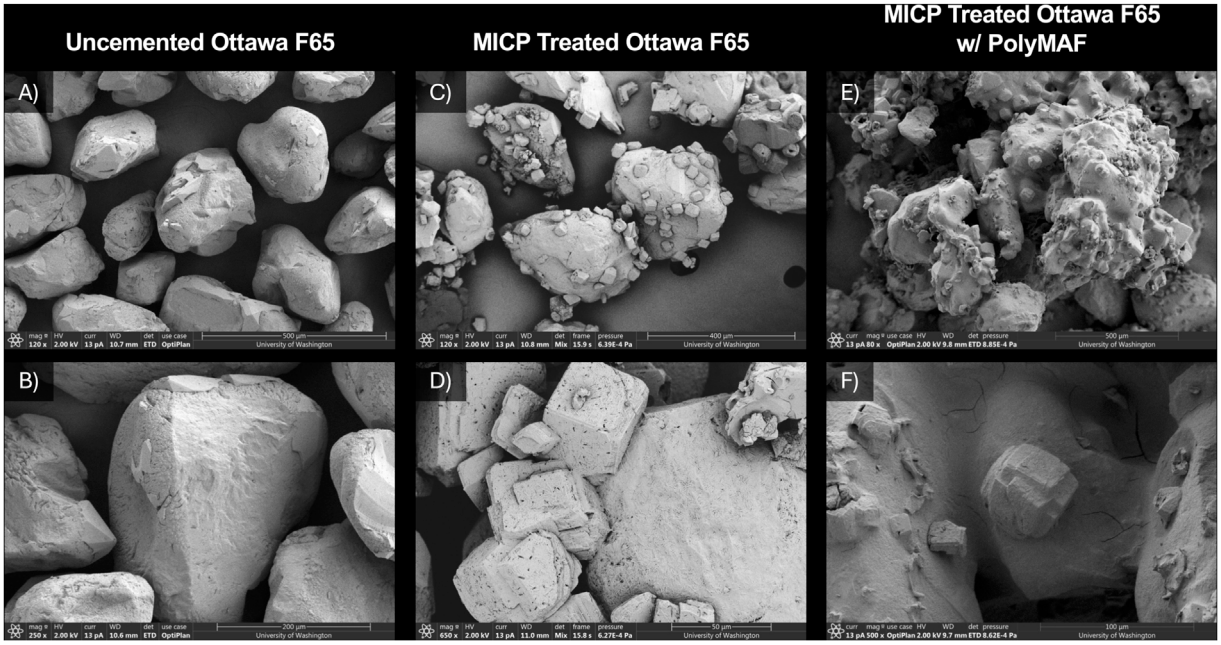

FIGURE 1
SEM images of intact soil subsamples from **(A,B)** Experiment 1 (Untreated Ottawa F65), **(C,D)** Experiment 2 (MICP Treated Ottawa F65), and **(E,F)** Experiment 3 (MICP Treated Ottawa F65 w/PolyMAF).

Experiments 1 through 3. As shown in Experiment 1 (Figures 1A,B), subangular particle morphologies were observed and untreated sand particle surfaces were smooth and absent of mineral precipitates. Experiment 2 (Figures 1C,D) which received an MICP treatment, however, exhibited well defined rhombohedral crystal morphologies characteristic of calcite minerals with many $CaCO_3$ crystals near 50 microns in diameter. After applying a PolyMAF treatment after MICP, large changes in material morphology were observed. Experiment 3 (Figures 1E,F), which received a PolyMAF treatment after MICP, had an amorphous polymer film that was visible and coated both particle and $CaCO_3$ crystal surfaces. The resulting polymer film was expected and may have been stabilized by the release of calcium ions during mineral dissolution and the cross-linking of alginate and calcium ions to form a calcium alginate gel (Blandino et al., 1999). During the experiment, generated gas bubbles were observed in the PolyMAF solution and suggested that bubbles were likely retained within the calcium alginate gel film. However, it remained unclear how this layer could be effectively incorporated within a biocemented composite.

Series 2 experiments

Series 2 experiments investigated the potential of secondary cementation treatments to entrap gases within composites by coating polymer films following PolyMAF treatments with additional calcium carbonate minerals. Tests specifically investigated the effect of PolyMAF treatments on subsequent mineral precipitation events as well as the impact of added magnesium during the second cementation treatment on precipitate formation. Figure 2 provides SEM images of intact soil subsamples from Experiments 4 through 7. When comparing Experiment 4 (Figures 2A,B) and 5 (Figures 2C,D) to Experiment 2 (Figures 1C,D) which had only one cementation treatment, the impact of the PolyMAF treatment on subsequent cementation formation can be observed. In both Experiment 4 and 5, more abundant calcium carbonate crystals were observed when compared to Experiment 2. In addition to the larger crystals that were expected after the first cementation treatment, smaller crystals were also observed in these samples and appeared to be more randomly distributed. This may have resulted in part from the second augmentation event which applied additional ureolytic cells before the secondary cementation treatment. When comparing Experiment 4 to 5, the effect of the PolyMAF treatment was less pronounced than expected. However, $CaCO_3$ crystals in Experiment 5 appeared to be somewhat larger and grouped together in larger clusters, possibly indicating that the polymer film had some effect on the nucleation of crystals during the secondary cementation treatment. Additional $CaCO_3$ formed in Experiment 5 during the secondary cementation treatment also did not appear to coat existing $CaCO_3$ surfaces, suggesting that polymer films were not likely retained within cementation. When magnesium ions were added to the secondary cementation treatment, however, large changes in material morphologies were observed with rougher and more amorphous mineral coatings appearing to exist preferentially on crystals previously established during the first cementation event (Figures 2E–H). The ability of magnesium additions to promote the coating of polymer films which existed on previous $CaCO_3$ crystals afforded the possibility to retain gases within these materials and appeared to result in both Experiment 6 and 7 at the 50 mM and 250 mM magnesium concentrations.

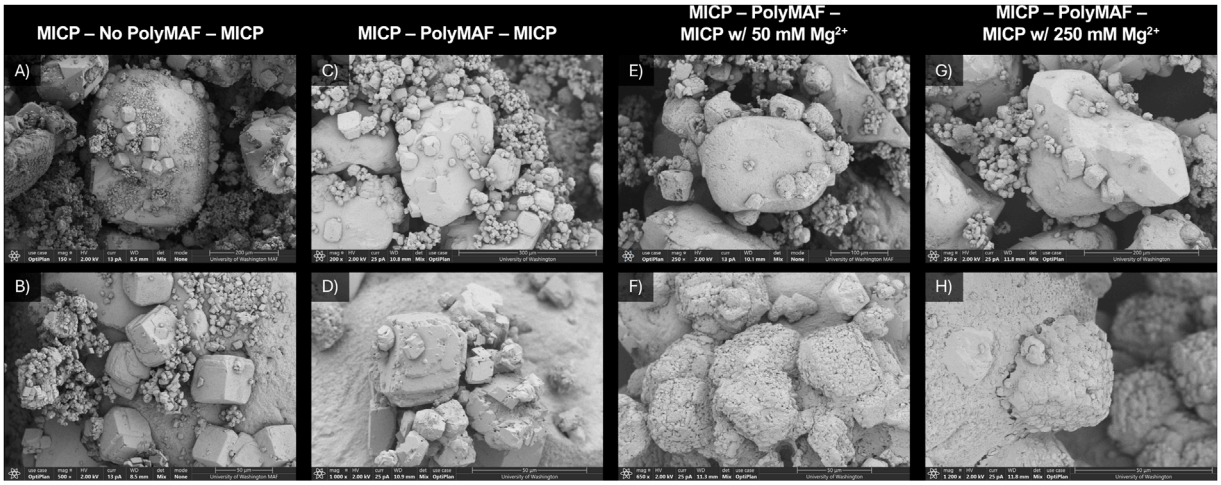

FIGURE 2
SEM images of intact soil subsamples from **(A,B)** Experiment 4 (MICP–No PolyMAF–MICP), **(C,D)** Experiment 5 (MICP–PolyMAF–MICP), **(E,F)** Experiment 6 (MICP–PolyMAF–MICP w/50 mM Mg^{2+}), and **(G,H)** Experiment 7 (MICP–PolyMAF–MICP w/250 mM Mg^{2+}).

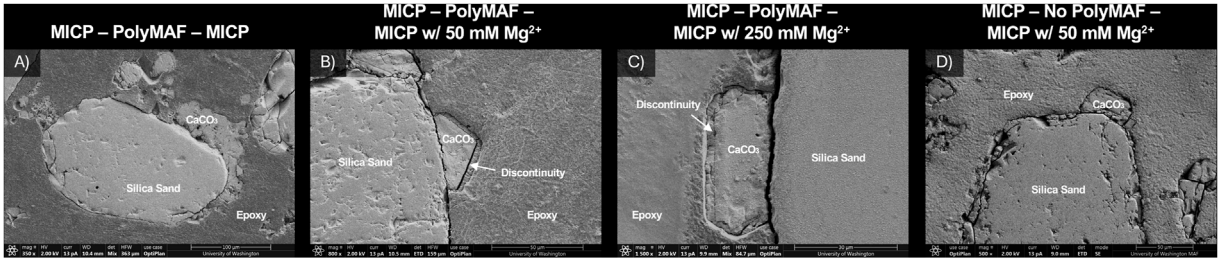

FIGURE 3
SEM images of epoxied soil cross-sections from **(A)** Experiment 5 (MICP–PolyMAF–MICP), **(b)** Experiment 6 (MICP–PolyMAF–MICP w/50 mM Mg^{2+}), **(c)** Experiment 7 (MICP–PolyMAF–MICP w/250 mM Mg^{2+}), and **(d)** Experiment 8 (MICP–No PolyMAF–MICP w/50 mM Mg^{2+}).

For select experiments, soil subsamples were embedded in epoxy and cross sectioned using a slow saw to reveal the internal structure of generated precipitates. Figure 3 provides SEM images of material cross-sections from Experiments 5 through 8. As shown in Experiment 5 (Figure 3A), cross sections revealed both the soil particle and calcium carbonate internal structures. $CaCO_3$ crystals appeared to be uniform in internal structure with minimal voids observed in crystals beyond some fractures resulting from the sawing process. Smaller $CaCO_3$ crystals also appeared to be clustered with larger $CaCO_3$ crystals with some voids existing in between these forms. However, when magnesium was added during secondary cementation, $CaCO_3$ crystals had a visible discontinuity near their surface that was expected to have resulted from the PolyMAF treatment with additional minerals present above this zone resulting from the magnesium amended cementation coating (Figures 3B,C). The discontinuity appeared to include small voids and fractured more readily during the sawing process suggesting that gases were likely retained within the biocemented composites. Again, no large changes were observed with changes in magnesium concentrations with similar discontinuities existing on crystals from both Experiment 6 and 7. In Experiment 8 (Figure 3D), which received a standard cementation treatment followed by a magnesium amended secondary cementation treatment, but no PolyMAF, crystal discontinuities were not observed suggesting again that this discontinuity resulted from the presence of the polymer film and entrapped gases and was not simply the result of the magnesium amended coating. Although promising, future characterizations should more definitively characterize the magnitude, location, and presence of gases within this polymer film to rule out other possible explanations for the observed artifacts.

In order to further investigate if magnesium additions were responsible for the improved coating of polymer layers on $CaCO_3$ crystals from the first cementation event, SEM-EDS analysis of a subsample from Experiment 6 was performed to determine elemental spatial abundances. As shown in Figure 4, a sand particle surface with calcium carbonate crystals suspected to be coated by the magnesium amended secondary cementation treatment was scanned. EDS elemental maps highlighted the presence of oxygen on the entire scanned section (Figure 4B), as expected, and confirmed the presence of both silica sand (Figure 4C) and $CaCO_3$ crystal surfaces (Figure 4E). When examining magnesium (Figure 4F) and chloride (Figure 4D) concentrations, higher magnesium

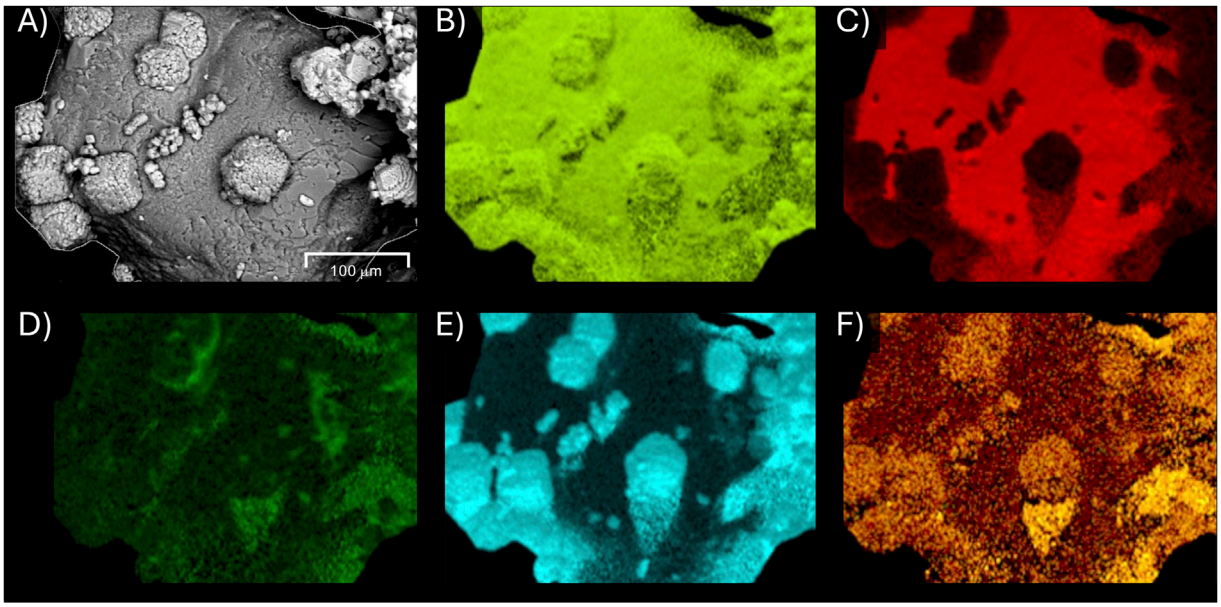

FIGURE 4
SEM-EDS images of biocemented sand surface from Experiment 6 (MICP–PolyMAF–MICP w/50 mM Mg^{2+}) showing **(A)** raw SEM image and elemental surface concentrations of **(B)** oxygen, **(C)** silica, **(D)** chloride, **(E)** calcium, and **(F)** magnesium.

appeared to be localized on existing $CaCO_3$ crystals supporting previous hypotheses that it promoted the coating of existing crystal surfaces following the PolyMAF treatment. Chloride concentrations were only slightly elevated on the surface of the sand and around these crystals suggesting that the observed crystal coatings were not solely the re-precipitation of added magnesium chloride, but rather magnesium ions were likely coprecipitated with $CaCO_3$ on these surfaces.

Conclusion

Experiments performed in this study suggested that biocemented composite materials with entrapped gases can be generated using novel treatment techniques. In our study, sands were first biocemented with a polymer treatment and microbial mixed acid fermentation activity was used to generate carbon dioxide gases as fermentation byproducts and chemically degrade calcium carbonate. The presence of sodium alginate biopolymers appeared to enable the retention of gases within a polymer film on the surface of previously generated calcium carbonate crystals. As biocementation was dissolved during the polymer treatments, released calcium ions were suspected to enable the formation of a calcium alginate gel that improved gas retention within the polymer film. When a secondary cementation treatment without magnesium was applied, smaller calcium carbonate crystals were generated and appeared to be widely distributed throughout samples. When magnesium chloride was provided in the secondary cementation treatment, however, nucleated crystals appeared to preferentially precipitate on existing $CaCO_3$ crystal and polymer film surfaces. Material cross section samples from experiments receiving PolyMAF treatments with a secondary cementation treatment containing magnesium demonstrated a visible discontinuity between calcium carbonate crystals and the magnesium amended cemented coating at the location of the polymer film. At this discontinuity, voids were observed suggesting that the polymer film retained gas bubbles that were successfully coated with the magnesium amended cementation layer. While the obtained results are promising, further work is needed to further characterize the presence, size, and spatial locations of generated gas inclusions within these biocemented composites and investigate their impact on soil undrained shearing behaviors.

Data availability statement

The raw data supporting the conclusions of this article will be made available by the authors, without undue reservation.

Author contributions

MG: Conceptualization, Funding acquisition, Methodology, Project administration, Resources, Supervision, Visualization, Writing – original draft, Writing – review and editing. EM: Data curation, Investigation, Methodology, Writing – original draft. BR: Methodology, Writing – review and editing. C-ET: Methodology, Writing – review and editing.

Funding

The author(s) declare that financial support was received for the research and/or publication of this article. Funding for this research

is provided by the National Science Foundation (NSF) grant no. ECI-2045058. Presented SEM and EDS images were made possible by the Molecular Analysis Facility, a National Nanotechnology Coordinated Infrastructure site at the University of Washington that is supported in part by the National Science Foundation Grants NNCI-1542101 and NNCI-2025489, the University of Washington, the Molecular Engineering and Science Institute, and the Clean Energy Institute. Any opinions, findings, conclusions, or recommendations expressed in this document are those of the author and do not necessarily reflect the views of the National Science Foundation or other funding sources.

Conflict of interest

The authors declare that the research was conducted in the absence of any commercial or financial relationships that could be construed as a potential conflict of interest.

Generative AI statement

The author(s) declare that no Generative AI was used in the creation of this manuscript.

Any alternative text (alt text) provided alongside figures in this article has been generated by Frontiers with the support of artificial intelligence and reasonable efforts have been made to ensure accuracy, including review by the authors wherever possible. If you identify any issues, please contact us.

Publisher's note

References

Blandino, A., Macías, M., and Cantero, D. (1999). Formation of calcium alginate gel capsules: influence of sodium alginate and CaCl2 concentration on gelation kinetics. *J. Biosci. Bioeng.* 88 (6), 686–689. doi:10.1016/S1389-1723(00)87103-0

Burdalski, R. J., Ribeiro, B. G. O., Gomez, M. G., and Gorman-Lewis, D. (2022). Mineralogy, morphology, and reaction kinetics of ureolytic bio-cementation in the presence of seawater ions and varying soil materials. *Sci. Rep.* 12 (1), 17100. doi:10.1038/s41598-022-21268-3

Carey, T. J., Stone, N., and Kutter, B. L. (2020). Grain size analysis and maxi-mum and minimum dry density testing of Ottawa F-65 sand for LEAP- UCD-2017. In: Kutter, B. L., Manzari, M. T., Zeghal, M., editors. *Model tests and numerical simulations of liquefaction and lateral spreading*. Cham: Springer International Publishing. p. 31–44.

DeJong, J. T., Mortensen, B. M., Martinez, B. C., and Nelson, D. C. (2010). Bio-mediated soil improvement. *Ecol. Eng.* 36 (2), 197–210. doi:10.1016/j.ecoleng.2008.12.029

DeJong, J. T., Soga, K., Kavazanjian, E., Burns, S., Van Paassen, L., Al Qabany, A., et al. (2013). Biogeochemical processes and geotechnical applications: progress, opportunities and challenges. *Géotechnique* 63 (4), 287–301. doi:10.1680/geot.sip13.p.017

DeJong, J. T., Gomez, M. G., San Pablo, A. C., Graddy, C. M. R., Nelson, D. C., Lee, M., et al. (2022). State of the art: MICP soil improvement and its application to liquefaction hazard mitigation. In: *Proceedings of the 20th ICSMGE-state of the art and invited lectures*. Alexandria, VA: National Science Foundation.

Feng, K., and Montoya, B. M. (2016). Influence of confinement and cementation level on the behavior of microbial-induced calcite precipitated sands under monotonic drained loading. *J. Geotechnical Geoenvironmental Eng.* 142 (1), 04015057. doi:10.1061/(ASCE)GT.1943-5606.0001379

Ferris, F. G., Stehmeier, L. G., Kantzas, A., and Mourits, F. M. (1997). Bacteriogenic mineral plugging. *J. Can. Petroleum Technol.* 36 (09). doi:10.2118/97-09-07

Gomez, M. G., Muchongwe, S. T., and Graddy, C. M. R. (2023). Biomediated control of colloidal silica grouting using microbial fermentation. *Sci. Rep.* 13 (1), 14184. doi:10.1038/s41598-023-41402-z

He, J., Chu, J., and Ivanov, V. (2014). Mitigation of liquefaction of saturated sand using biogas. In: *Bio-and chemo-mechanical processes in geotechnical engineering: géotechnique symposium in print 2013*. London, England: ICE Publishing. p. 116–124.

Lee, M., and Gomez, M. G. (2024). Liquefaction triggering and post-triggering behavior of biocemented loose sand. *Can. Geotechnical J.* 61 (7), 1331–1352. doi:10.1139/cgj-2023-0132

Mitchell, J. K., and Kelly, R. (2013). Addressing some current challenges in ground improvement. *Proc. Institution Civ. Eng. - Ground Improv.* 166 (3), 127–137. doi:10.1680/grim.12.00030

Montoya, B. M., and DeJong, J. T. (2015). Stress-strain behavior of sands cemented by microbially induced calcite precipitation. *J. Geotechnical Geoenvironmental Eng.* 141 (6), 04015019. doi:10.1061/(ASCE)GT.1943-5606.0001302

Okamura, M., and Soga, Y. (2006). Effects of pore fluid compressibility on liquefaction resistance of partially saturated sand. *Soils Found.* 46 (5), 695–700. doi:10.3208/sandf.46.695

O'Donnell, S. T., Rittmann, B. E., and Kavazanjian, E. (2017). MIDP: liquefaction mitigation *via* microbial denitrification as a two-stage process. I: desaturation. *J. Geotechnical Geoenvironmental Eng.* 143 (12), 04017094. doi:10.1061/(ASCE)GT.1943-5606.0001818

Pham, V. P., Van Paassen, L. A., Van Der Star, W. R. L., and Heimovaara, T. J. (2018). Evaluating strategies to improve process efficiency of denitrification-based MICP. *J. Geotechnical Geoenvironmental Eng.* 144 (8), 04018049. doi:10.1061/(ASCE)GT.1943-5606.0001909

Sorenson, K., Preciado, A. M., Moug, D., Khosravifar, A., Van Paassen, L., Kavazanjian, E., et al. (2022). Field monitoring of the persistence of microbially induced desaturation for mitigation of earthquake induced soil liquefaction in silty soil. *Lifelines* 2022, 101–113. doi:10.1061/9780784484449.009

Stocks-Fischer, S., Galinat, J. K., and Bang, S. S. (1999). Microbiological precipitation of CaCO3. *Soil Biol. Biochem.* 31 (11), 1563–1571. doi:10.1016/S0038-0717(99)00082-6

Van Paassen, L. A., Daza, C. M., Staal, M., Sorokin, D. Y., Van Der Zon, W., and Van Loosdrecht, M. C. M. (2010). Potential soil reinforcement by biological denitrification. *Ecol. Eng.* 36 (2), 168–175. doi:10.1016/j.ecoleng.2009.03.026

Zeng, C., Van Paassen, L. A., Zheng, J., Stallings Young, E. G., Hall, C. A., Veenis, Y., et al. (2022). Soil stabilization with microbially induced desaturation and precipitation (MIDP) by denitrification: a field study. *Acta Geotech.* 17 (12), 5359–5374. doi:10.1007/s11440-022-01721-3